Compressed Sensing CPMG with Group-Sparse Reconstruction for Myelin Water Imaging

H. S-M. Chen[1], A. Majumdar[2], and P. Kozlowski[1,3]
[1]UBC MRI Research Centre, Vancouver, BC, Canada, [2]Electrical and Computer Engineering, University of British Columbia, Vancouver, BC, Canada, [3]ICORD, Vancouver, BC, Canada

Introduction

Myelin content is an important marker for central nervous system pathology. Myelin water imaging has been shown to measure myelin content in normal and diseased brain and spinal cord tissue [1, 2]. One way to generate myelin water map is to utilize multi-echo CPMG sequence. However, CPMG is inherently a slow sequence, which is especially true in *in vivo* small mammal studies with conflicting requirements of very high SNR and spatial resolution and reasonably short scan time. To improve the acquisition efficiency, this study investigates the use of compressed sensing (CS) to accelerate myelin water measurement.

Multi-echo CPMG produce series of differently T2 weighted images in the same anatomical volume. Rather than just exploiting the spatial correlations within each image (sparsity in wavelet domain), we chose to exploit the correlations among the images (group-sparsity) as well. This makes image reconstructed with high accuracy from significantly fewer *k*-space samples possible. We hypothesize that using CS multi-echo CPMG with group-sparse reconstruction will significantly increase the acquisition efficiency of myelin water images.

Methods

All MRI experiments were carried out on a 7 T animal scanner (Bruker, Germany). Single slice multi-echo CPMG sequence was used to acquire fully sampled *k*-space data from an excised rat cervical spinal cord sample using a 13 mm i.d. solenoid coil (256 × 256 matrix, TE/TR = 1500/6.738 ms, 32 echoes, 2.56 cm FOV, 1 mm slice, NA = 6, 4) [3]. Undersampled *k*-space data was generated for different acceleration factors (1.5, 2, 4, 5.3, 8), with 33% of the read-out lines placed around the centre of the *k*-space, and the rest randomly placed in the outer region. Different sampling patterns were used for each echo to prevent constructive aliasing interferences and further enforce sparsity. Group-sparse reconstruction was performed using SPGL1 [4]. Non-negative least square (NNLS) analysis was used to calculate the T2 distribution [5]. Myelin water fraction maps were generated by dividing the integral from 7.75–20 ms range by the total integral of the T2 distribution.

Results and Discussion

Table 1. NMSE over the entire acquisition volume for all 32 echo-images between the sparsely sampled dataset and the fully sampled dataset.

Acceleration factor	8	5.3	4	2	1.5
Number of read-out lines	**32**	**48**	**64**	**128**	**170**
NMSE	0.30	0.16	0.085	0.047	0.036

Table 2. NMSE and correlation coefficient between the MWF generated from sparsely sampled and the fully sampled datasets in rat spinal cord.

Acceleration factor	4	2	1.5
Number of read-out lines	**64**	**128**	**170**
Correlation Coefficient	0.64	0.91	0.97
NMSE	0.43	0.20	0.10

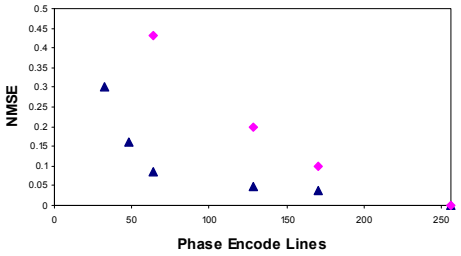

Figure 1. NMSE versus phase encode lines per echo image, pink denotes errors in MWF, and blue denotes errors in the echo images. Note that NMSE is zero at 256 because all points are undersampled from the same dataset.

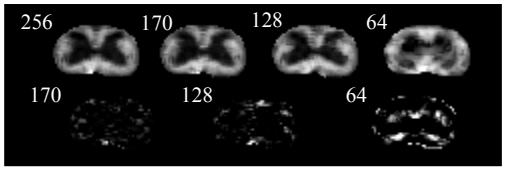

Figure 2. Top row shows MWF at various acceleration factors, with grey scale from 0 to 0.5. Bottom row shows difference image between accelerated and unaccelerated MWF. Number denotes phase encode lines per echo image. Grey scale from 0 to 0.2. NA=6.

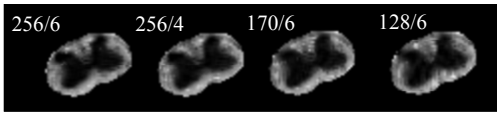

Figure 3. MWF maps obtained at various averages and acceleration factors. Numbers are phase encodes per echo image/NA. Colour scale is from 0 to 0.5

Table 1 shows the normalized mean square error (NSME) in the entire slice for all 32 echo-images between the accelerated and unaccelerated dataset, *i.e.* the ground truth. NSME remains small below acceleration factor of 4 (64 phase encoding steps), but increases quickly beyond that (Fig. 1, blue). Table 2 shows the NMSE and correlation coefficient in MWF maps in the spinal cord between the sparsely sampled dataset and the fully sampled dataset. Unlike the echo-images, NSME in MWF increases rapidly with acceleration factor (Fig 1, pink). Figure 2 shows MWF maps and difference images at various simulated accelerations from the same dataset. MWF map quality remained adequate at 2 times acceleration, with the largest error contributors at the periphery, where the sample interfaces with the fixative solution.

Figure 3 shows MWF maps obtain at various averages and acceleration factors. Each dataset was a separate acquisition. Acquisition time for 1.5 times acceleration MWF map with 6 averages and unaccelerated MWF map at NA = 4 are the same. There is little difference in the quality of MWF map. The result for 2 times acceleration at six averages is especially encouraging; it demonstrates that high acquisition efficiency is possible with CS CPMG. The improve in efficiency is expected to be even greater in low SNR situations, such a as *in vivo* rat spinal cord studies. Due to the nature of NNLS analysis we are using, at six averages with the solenoid coil on an excised cord, we were already above the SNR where little improvement is seen in MWF map quality. Therefore the unaccelerated data at 4 NA versus accelerated data at 6 NA is more representative of the improvement that can be made.

It remains to be found a balance between the number of averages and acceleration factor in order to achieve the highest possible efficiency in myelin water measurement using this particular method. Better probability density function for the sampling scheme could also improve image quality and will be investigated.

Conclusions

CS multi-echo CPMG with group-sparse reconstruction is a promising approach at increasing acquisition efficiency in myelin water mapping.

Acknowledgements

This study has been supported by the Canadian Institutes of Health Research.

References:

[1] Laule C, et al. J Neurol, 2004, **251**,284;
[2] Kozlowski P, et al., Magn Reson Med, 2008, **59**, 796;
[3] Poon CS, *et al*. J Magn Reson Imaging, 1992, **2**, 541;
[4] van den Berg E *et al.*, SIAM J on Sci Comp, 2008, **31**:890;
[5] Whittall KP, et al. Magn Reson Med, 1997, **37**, 34;